

FoldNet: Learning Generalizable Closed-Loop Policy for Garment Folding via Keypoint-Driven Asset and Demonstration Synthesis

Yuxing Chen^{1,2}, Bowen Xiao^{1,2}, He Wang^{1,2,3,†}

¹CFCS, School of Computer Science, Peking University ²Galbot

³Beijing Academy of Artificial Intelligence

[†]Corresponding Author: hewang@pku.edu.cn

Abstract: Due to the deformability of garments, generating a large amount of high-quality data for robotic garment manipulation tasks is highly challenging. In this paper, we present a synthetic garment dataset that can be used for robotic garment folding. We begin by constructing geometric garment templates based on keypoints and applying generative models to generate realistic texture patterns. Leveraging these keypoint annotations, we generate folding demonstrations in simulation and train folding policies via closed-loop imitation learning. To improve robustness, we propose KG-Dagger, which uses a keypoint-based strategy to generate demonstration data for recovering from failures. KG-Dagger significantly improves the model performance, boosting the real-world success rate by 25%. After training with 15K trajectories (about 2M image-action pairs), the model achieves a 75% success rate in the real world. Experiments in both simulation and real-world settings validate the effectiveness of our proposed framework.

Keywords: Synthetic Dataset, Garment Manipulation, Imitation Learning

1 Introduction

Garment manipulation has been widely studied in robotics [1]. However, due to the deformable nature of garments, such tasks remain highly challenging. In recent years, data-driven learning approaches have made significant progress, with imitation learning [2] gradually emerging as the main paradigm for the acquisition of various robotic skills. Several improved variants of imitation learning have been explored in the literature [3, 4, 5, 6, 7]. However, applying imitation learning to garment manipulation tasks remains significantly hindered by the scarcity of high-quality data.

Learning from synthetic data has become an efficient approach for robot learning [8, 9, 10]. Many datasets [11, 12, 13] and simulation environments [14, 15] are now available to generate garment manipulation data. In simulation, it is possible to flexibly modify both the environment and the properties of the garments, allowing stronger generalization capabilities. However, improving the quality of synthetic data remains a key challenge. Current methods face two main limitations:

Limited garment assets and lack of detailed annotations. Existing datasets often contain only a small number of garment meshes and lack rich annotations. This limited data availability imposes an upper bound on generalization performance. Moreover, the lack of detailed annotations requires researchers to put in extra effort to generate high-quality demonstration data in simulation.

Limited handling of error recovery. Garment manipulation tasks are long-horizon tasks that involve complex deformable object dynamics. Compared to previously dominant open-loop approaches for garment manipulation [8, 16], closed-loop control offers the potential to retry after failures. However, if training data only contains perfect demonstrations, small errors at each step can accumulate and potentially cause the garment to enter previously unseen states, often resulting in task failure. This poses a significant challenge for learning robust policies.

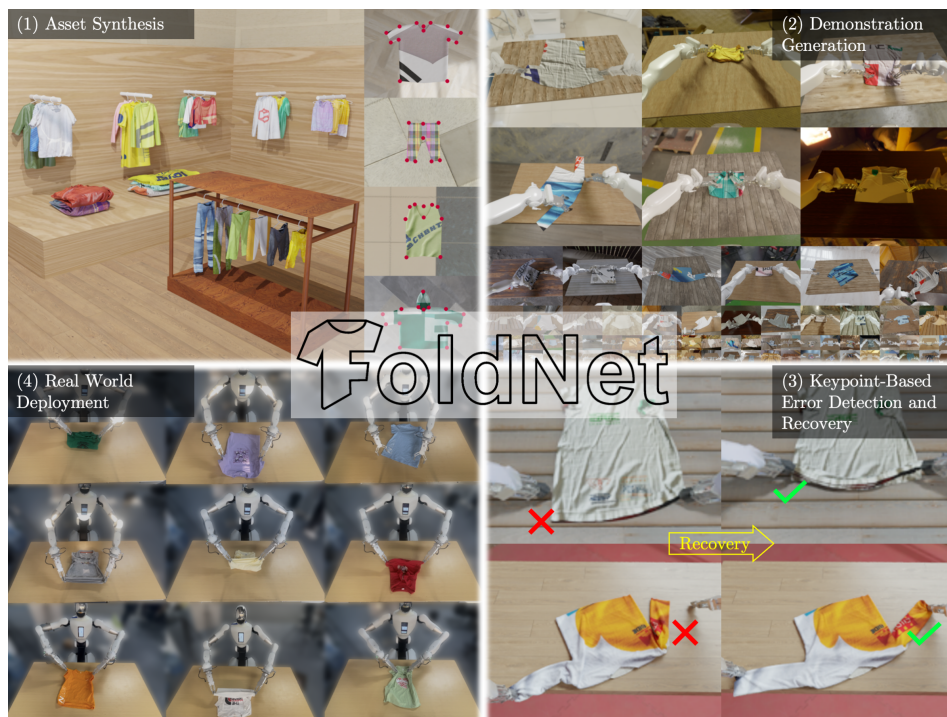


Figure 1: **FoldNet** consists of four main components: (1) asset synthesis, (2) demonstration generation, (3) keypoint-based error detection and recovery, and (4) real world deployment.

To address the scarcity of garment assets, we propose a garment mesh generation framework. For each category of garment, we design a template whose geometry is controlled by a set of keypoints. We then apply generative models to synthesize texture maps for garments. This approach enables scalable garment mesh generation, and each mesh is accompanied by automatically generated keypoint annotations for subsequent demonstration generation and policy learning.

To handle out-of-distribution states, we introduce Keypoint-Gated DAgger (KG-DAgger). After training the initial policy network, we run the policy and use the previously automatically annotated keypoints to detect potential failure cases. When a failure is detected, a keypoint-based strategy is invoked to perform a correction. The corrected trajectories are then added to the dataset for further policy training.

In summary, this work makes the following two key contributions:

- 1) We propose a garment mesh generation framework that can automatically produce highly diverse garment meshes with annotated keypoints.
- 2) We introduce KG-DAgger, boosting the success rate of closed-loop folding in the real world from 50% to 75%.

2 Related Works

2.1 Garment Manipulation

Garment manipulation is a widely studied task in robotics [1]. Many works focus on garment folding [16, 17, 13] and unfolding [8, 18]. The main challenges lie in the deformable nature of garments and their complex dynamics. Various approaches have been explored to address these challenges, including imitation learning [17], reinforcement learning [9], model-based methods [19, 20], etc. However, how to train closed-loop garment manipulation models using synthetic data has rarely been explored. In this work, we focus on the task of robotic garment folding using closed-loop imitation learning.

Dataset	Garments	Category	RGB	Multi-layer ¹	SK ²	Resolution
ClothesNet [12]	3.1K	11	✓	✓	✗	1 cm
Cloth3D [11]	11.3K	4	✗	✓	✗	1 cm
aRTF [13]	10K / Day ^{3,4}	3	○ ⁵	✗	✓	Adjustable
Ours	2K / Day ³	4	✓	✓	✓	Adjustable

Table 1: Comparison with other synthetic datasets. ¹The garment has both a front and a back layer. ²Semantic keypoint. ³The generation speed is estimated based on a single RTX 3090. ⁴Including the time for rendering. ⁵Although RGB is included, it lacks consistency with the clothing geometry.



Figure 2: **Synthetic garment meshes.** These static garment meshes can be used for subsequent physics simulation and policy learning.

2.2 Synthetic Garment Assets

Existing garment mesh datasets are typically designed manually by artists [12] or generated based on predefined templates [13, 21, 11]. Template-based methods allow for large-scale mesh generation, but additional texture maps are required to render garments with a realistic appearance. Previous methods either directly apply existing texture libraries to garment meshes [13], or use generative models to synthesize textures [22, 23, 24]. However, the textures generated by the former methods differ significantly from those of real garments, while the latter methods perform poorly when applied to garment meshes. In this work, we adopt a template-based strategy to generate garment geometry and design a pipeline utilizing generative models to produce more realistic textures.

2.3 Imitation Learning

In recent years, imitation learning [25, 26, 27, 28] has gained increasing attention from the research community. One of its key challenges is collecting high-quality demonstration data. Many works rely on human labor to collect demonstrations in the real world, including methods such as human labelling [18, 17], teleoperation [29, 30] or virtual reality [16]. Another approach is to learn in simulation, typically distilling from an expert policy [9, 31]. The recovery from errors [32, 33, 34] has become a topic of great interest in recent research. Our method performs imitation learning in simulation by distilling a keypoint-based policy into a vision-based model, while enhancing the robustness of the trained model by generating demonstrations that include recovery from failures.

3 Garment Mesh Synthesis

We compare our asset dataset with several existing synthetic datasets, as shown in Table 1. The pipeline for our method is shown in Figure 3. The main steps in our generation process include: (1) creating the geometry of the garment in 3.1, (2) generating the texture of the garment in 3.2, and (3) combining the geometry and texture and filtering in 3.3.

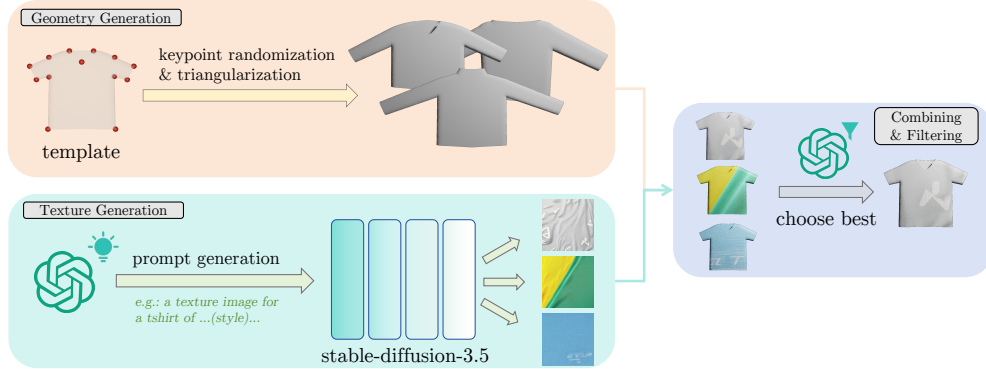


Figure 3: **Pipeline for garment mesh synthesis.** Through *geometry generation*, *texture generation*, *combining-and-filtering*, we can generate scalable high-quality garment meshes.

3.1 Geometry Generation

We use a template-based approach to generate garment geometry. For four types of garments — t-shirt (including long-sleeved and short-sleeved), vest (sleeveless), hoodie, and trousers — we design a specific template for each. These templates define the shape of the garment using the 2D positions (x, y) of keypoints on the garment. By randomizing the positions of the keypoints, we can generate a large variety of garment shapes. Once the keypoint positions are determined, we connect the control points using Bezier curves and perform triangulation within the xy -plane. Then, we heuristically define the z -coordinates and UV coordinates for the mesh vertices. During this process, keypoints are automatically annotated on the generated triangular mesh.

3.2 Texture Generation

To automatically generate garment textures, we use pre-trained generative models. First, for each type of garment, we use a large language model [35] to generate a description of the texture. Then, we use this description as a prompt for a Text2Image model [36]. Repetition of this process multiple times can quickly generate a large number of texture images.

3.3 Combining and Filtering

To enhance the consistency between texture images and garment meshes, we introduce an additional filtering step. For each garment mesh with only geometry, we combine it with different texture images and render the results. A vision language model [35] is then used to automatically select the most suitable texture as the final texture for that mesh.

4 Demonstration Generation

The training framework is illustrated in Figure 4. We begin by using a keypoint-based policy to generate the initial dataset for imitation learning. This dataset is then used to train a vision-action model. Subsequently, we use the inference result of the model to generate additional trajectories and employ a keypoint-based strategy for error recovery. Finally, we iterate the data generation loop of model training and model rollout, a process we refer to as KG-Dagger.

4.1 Keypoint-Based Policy

For each category of garment, we can design a simple keypoint-based policy for demonstration generation, as illustrated in Figure 5 (a). The initial grasping positions and target positions for each stage can be computed based on the ground-truth keypoint locations, while the intermediate positions are determined via interpolation. To generate demonstrations for different folding strategies, we can simply modify the initial and target positions at each stage.

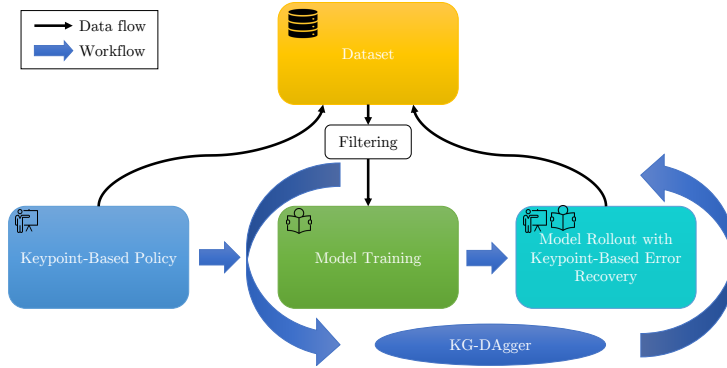


Figure 4: **Demonstration generation pipeline.** This figure illustrates the complete workflow and data flow of our demonstration data generation framework.

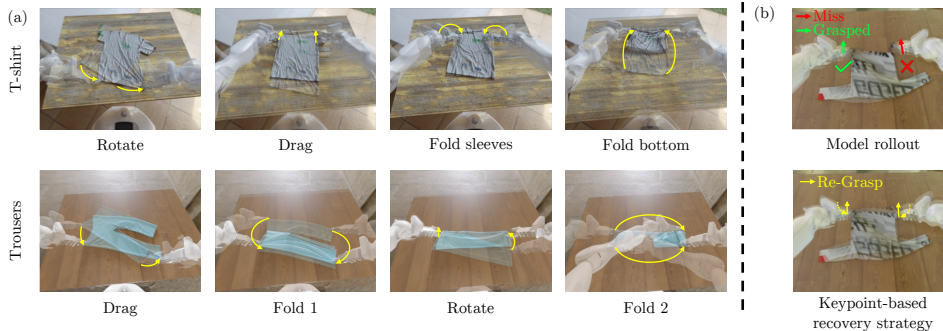


Figure 5: **(a) Keypoint-based policy.** The entire folding process can generally be broken down into several subtasks, which are then executed sequentially during the demonstration generation process. **(b) Keypoint-based recovery.** Our keypoint-based recovery strategy can generate error correction action automatically after a grasp failure is detected.

4.2 Model Training

We choose diffusion policy [37] as our vision-action model. We retain only successful trajectories and filter out failed ones for policy training. At the end of each trajectory, we pad several no-op actions to indicate termination.

4.3 Model Rollout with Keypoint-Based Error Recovery

KG-Dagger is similar to HG-Dagger [32]: during model inference, we use a keypoint-based strategy to detect grasp failures — a step that is performed by a human expert in HG-Dagger. This monitoring process leverages the keypoints of the garment at each time step, along with the gripper state. If grasp failure is detected, the keypoint-based recovery strategy takes over after a short delay and directs the gripper to the target keypoint, as illustrated in Figure 5 (b). The reason for this delay is that the vision-based model cannot detect a grasp failure at the moment of grasping; it must move the arm a certain distance before the failure can be detected from the visual input. After the keypoint-based correction, the model continues to predict actions. These trajectories, which include keypoint-based recovery, are also added to the dataset and used jointly for model training. During training, we assign a weight of 0 to actions that lead to grasp failures.

5 Experiments

We design two tasks to validate the effectiveness of our method: keypoint detection and garment folding. The keypoint detection task is easier to benchmark and demonstrates how closely the generated garment meshes match real-world garments. The garment folding task is more comprehensive and allows the evaluation of the quality of the generated demonstration data.



Figure 6: **Keypoint detection in the real world.** The figure shows the predicted output of our keypoint detection model on real images.

5.1 Keypoint Detection

5.1.1 Experiment Setup

Environment. In this experiment, the model is given an image and the category of the garment, and is required to predict the positions of all keypoints. We directly use the model architecture in [13] for keypoint detection. We use PyFlex [15] as the physics simulator and Blender [38] for rendering. By synthesizing garment images and keypoint annotations in simulation, we train a model to predict keypoints and then evaluate it on real-world images. We also assume that the mask is known and the background is masked out. In the real world, we use Grounded-SAM [39] for segmentation.

Metric. We select **Mean Average Precision (meanAP)** and **Average Keypoint Distance (AKD)** as metrics [13]. We model keypoint detection as a classification problem, and being correctly classified means the pixel-wise Euclidean distance between detected keypoints and ground truth keypoints is less than a given threshold. The thresholds in our experiment are 4-pixel and 8-pixel, each corresponds to about 0.5 cm and 1 cm in the real world. Given this definition, the meanAP is the proportion of keypoints that have been correctly classified, and the reported meanAP is the average of results under two thresholds. AKD is the average pixel-wise distance between predicted and ground truth keypoints. In the ground truth images, we only annotate the visible keypoints. For both metrics, invisible keypoints are ignored during the evaluation.

Asset. For each category of garment, we generate 1,500 instances of synthetic garments for training using our proposed asset generation pipeline. We collect a total of about 800 real-world images across all garments for testing.

5.1.2 Experiment Results

Category	mAP _{4,8} (↑)				AKD (↓)			
	Ours	w/o filter	aRTF	Paint-it	Ours	w/o filter	aRTF	Paint-it
T-Shirt	59.0	50.5	42.2	47.2	10.3	9.3	11.3	14.2
Trousers	51.7	57.0	47.4	47.8	16.9	16.4	14.1	32.0
Vest	42.5	43.5	26.0	37.3	20.0	16.7	17.3	43.7
Hoodie	35.7	32.3	31.0	29.5	19.8	20.1	18.9	35.9
Average	47.2	45.8	36.6	38.0	15.6	16.7	15.4	31.4

Table 2: The performance of keypoint detection models trained with different mesh generation methods. In the *Average* row, we highlight the best two columns in bold.

Different texture generation pipeline. We compare the performance of different garment texture generation methods. *Ours* refers to our complete method, *w/o filter* refers to our method without the final filtering stage, *aRTF* refers to the method from [13], and *Paint-it* refers to the method from [22]. The experimental results are shown in Table 2. Compared to previous methods, our framework performs well on both the meanAP and AKD metrics. The ablation study also demonstrates that the final VLM-based filtering step is effective.

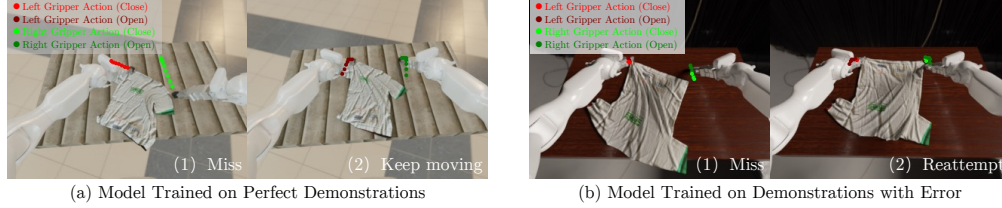


Figure 7: Comparison of folding policy in simulation.

5.2 Folding Policy Learning

5.2.1 Experiment Setup

Environment. We use PyFlex [15] as our physics simulator and Blender [38] for rendering. The initial state of the garment includes random rotation around the z-axis (vertical axis), random flipping, and some randomly generated wrinkles. We use the RGB from the robot’s head-mounted D436 camera as the single-view visual input. The complete action space consists of the XYZ coordinates of both grippers, as well as the gripper’s open-close state, resulting in a total of 8 dimensions. We assume that the height of the table is known and fixed.

Each demonstration trajectory has a length of around 120 steps. During testing, a trajectory is considered terminated if it exceeds 300 steps or if the movement distance between consecutive actions is less than 1 mm.

Metric. To automatically determine the success of folding in simulation, we first run the keypoint-based policy on a perfectly initialized garment configuration. We refer to the resulting garment mesh as $mesh_{gt}$. During model evaluation, we compare the final folded mesh $mesh_{eval}$ with $mesh_{gt}$. After aligning the two meshes with an arbitrary rigid-body rotation and translation, folding is considered successful if the average vertex-wise error is below 0.4 mm. In the real world, the success of folding is determined by human experts.

Asset. For each category of garment, we generate 1,000 training instances using our proposed asset generation pipeline. During testing, we use an additional set of 100 previously unseen garments. For the background of the table and the scene, we randomly sample a collection of indoor assets downloaded from PolyHaven [40]. For real-world testing, we use 10 unseen garments.

5.2.2 Experiment Results

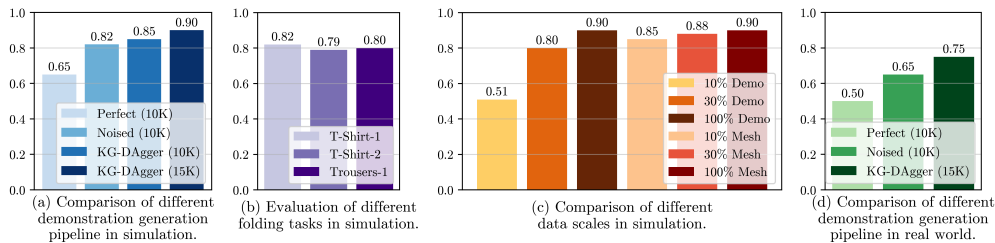


Figure 8: Experiment results of garment folding.

Different demonstration generation pipeline. In Figure 8(a), we first compare the performance of models trained with different demonstration data generation pipelines in simulation. *Perfect* refers to using only perfect demonstrations, *Noised* refers to using only demonstrations with added noise [10]. This baseline also uses the keypoint-based error recovery strategy to augment the dataset, but differs from KG-DAgger in that the actions are generated by adding noise to the ground-truth actions before execution, rather than using actions predicted by the network. *KG-DAgger* corresponds to the complete method in Section 4. The numbers in parentheses indicate the total number of training trajectories used. *KG-DAgger(15K)* represents the complete dataset, *KG-DAgger(10K)* is a sub-



Figure 9: **Real world deployment.**

set sampled from it with 10K trajectories, used for comparison under the same number of training demonstrations.

When the dataset includes trajectories with error corrections (*Noised*, *KG-Dagger*), there is a significant performance improvement compared to using only perfect demonstrations (*Perfect*). Figure 7 illustrates this difference: the model trained only on perfect demonstrations fails to retry after a grasp failure, whereas the model trained with error recovery data can do so. *KG-Dagger* method further narrows the gap between the data distribution during training and that during testing compared to *Noised* method, resulting in better performance.

Different tasks. Our data generation pipeline can be adapted to various folding patterns. In Figure 8(b), we use 10K trajectories generated by the *Noised* method as training data. The folding procedures for *T-Shirt-1* and *Trousers-1* are illustrated in Figure 5(a). The difference between *T-Shirt-2* and *T-Shirt-1* lies in the final step: instead of folding the bottom of the shirt upwards, *T-Shirt-2* folds it from left to right.

Data scale. We compare the performance of the model when trained with different numbers of garments and demonstrations, as shown in Figure 8(c). Here, 100% usage indicates training with 1000 garments and 15K demonstrations. When the amount of data reaches this scale, the model can achieve good performance in the simulator.

Sim2real performance. Our trained model can be directly transferred from simulation to the real world. As shown in Figure 8(d), we compare the real-world performance of the model trained with different demonstration generation methods. The model trained with our *KG-Dagger* approach performs better than the one trained with other demonstration data. Some examples of model outputs in the real world are shown in Figure 9.

6 Conclusion

In this paper, we present a synthetic dataset for garment folding. At the core of the dataset are garment keypoints, which enable both the synthesis of garment meshes and the generation of demonstration data. To further improve model performance, we incorporate keypoint-based error recovery data into the demonstration dataset. Our experiments show that models trained with this dataset can be directly transferred to real robots and unseen garments.

7 Limitation

Currently, the folding patterns are relatively simple, mainly due to limitations in the physical realism of the cloth simulation. When more complex folding methods are adopted, the realism of the simulation significantly degrades. In the future, the use of finer cloth meshes and more efficient and accurate simulators could further reduce the sim-to-real gap. Exploring the addition of rotational degrees of freedom in the action space is also a promising direction. In addition, combining synthetic and real-world data has the potential to improve success rates in the real world.

Acknowledgments

We thank Galbot for providing computational resources and robotic platforms. We thank Yufei Ding for her help with asset synthesis in the early stages of the project.

A Asset Synthesis Detail

In our data generation pipeline, creating a mesh template is very fast. Deforming a mesh using PyFlex takes approximately 6 seconds, and generating a texture image with Stable-Diffusion-3.5 requires around 20 seconds (excluding waiting for ChatGPT responses). Rendering a 480×720 image takes about 2 seconds. Overall, it takes roughly 30 seconds to generate a single cloth instance. All experiments are conducted on a server equipped with two Intel Xeon Platinum 8255C CPUs (48 cores, 96 threads, 2.50 GHz base frequency) and an NVIDIA RTX 3090 GPU.

B Comparison with Other Asset Generation Methods



Figure 10: Qualitative results of different generation pipelines.

C Keypoint Detection Detail

Category	# scenes		# cloth items	
	Train	Test	Train	Test
T-Shirt	207	1	1500	480
Trousers	207	1	1500	82
Vest	207	1	1500	96
Hoodie	207	1	1500	96
Total	207	1	6000	754

Table 3: Composition of dataset for keypoint detection.

We detect keypoints on 480×720 input images. The keypoint coordinates are converted into Gaussian blobs on 2D probability heatmaps, which serve as targets for pixel-wise logistic regression with

a binary cross-entropy loss. Our model adopts a U-Net [41]-inspired architecture, with a pretrained MaxViT [42] nano model from the Timm library [43] as the encoder. The network takes a 480×720 RGB image and its corresponding garment mask as input and outputs N heatmaps of size 256×256 , where N denotes the number of keypoints for the garment category. Keypoints are extracted from the predicted heatmaps by identifying local maxima within a 3×3 pixel window, using a probability threshold of 0.01. During training, we apply data augmentation techniques including color jittering, random rotation and translation, and random patching. The model is trained for 5 hours per category on a single NVIDIA RTX 3090 GPU.

D Real Asset for Garment Folding



Figure 11: Real world assets.

E Folding Simulation Environment

PyFlex uses Position Based Dynamics (PBD) for simulating clothing. We only consider the collisions between the clothing and the table, as well as the self-collisions of the clothing, ignoring the collisions between the clothing and the robot. The simulation of the grasping process uses *attachment*: when the gripper closes, if a particle of the clothing is very close to the gripper, it will be attached to the gripper until the gripper opens.

Parameter	Value
num_vert	~ 40k
num_face	~ 90k
step_dt	0.2 s
physics_dt	0.0025 s
num_solver_iter	20
grasp_th	0.02 m
particle_radius	adaptive
stiff_stretch	[1.5, 2.5]
stiff_bend	[0.015, 0.025]
cloth_table_fric	[0.75, 1.25]
cloth_cloth_fric	[0.75, 1.25]
tshirt_scale	[0.40, 0.50] m
trousers_scale	[0.45, 0.65] m

Table 4: Simulation parameters. $[x, y]$ denotes uniform sampling from the interval.

- **num_vert**: Number of vertices of the garment mesh.
- **num_face**: Number of faces of the garment mesh.

- **step_dt**: The time interval between two actions output by the policy.
- **physics_dt**: The time interval for physics simulation.
- **num_solver_iter**: Number of PBD solver iterations in PyFlex.
- **grasp_th**: Vertices within this range will be grasped when the gripper closes.
- **particle_radius**: The collision distance between cloth particles. This value is calculated as 1.5 times the average length of all edges.
- **stiff_stretch**: Stiffness of stretching.
- **stiff_bend**: Stiffness of bending.
- **cloth_table_fric**: The friction coefficient between the cloth and the table.
- **cloth_cloth_fric**: Self-collision friction coefficient of the cloth.
- **tshirt_scale**: Geometric mean of the tshirt’s span in the x and y directions.
- **trousers_scale**: Geometric mean of the trousers’s span in the x and y directions.

The simulation and rendering are computationally expensive, with high demands on both the CPU and GPU. We use AMD EPYC 7543 CPUs with 128 processors in total and 8 NVIDIA RTX 4090 GPUs to run the simulation and rendering. It takes approximately one day to generate 1,000 complete trajectories.

F Robot IK Solver

Our IK solver uses the Newton iteration method. The optimization objective includes three degrees of freedom for the translation of the end-effector and one degree of freedom for rotation (with the requirement that the gripper opens and closes parallel to the table, with no constraints on the other two rotational degrees of freedom). The optimized variables include the 7 degrees of freedom for each of the two arms.

The robot’s base and the table remain stationary. To extend the reachable range, we design the following method: based on the target positions for the two arm end-effectors, we calculate the joint angles of the legs such that the robot’s torso can move forwards and backwards, as well as rotate left and right. These algorithms are heuristic-based and designed to ensure robustness. As a result, the camera view on the head may experience small changes.

G Keypoint-Based Recovery

Figure 12 illustrates in detail how the keypoint-based error recovery is implemented. Overall, the recovery process consists of five sequential statuses. For each status, we show the observation at the beginning and the end. The three steps shown in each status are only illustrative — each phase may consist of multiple steps.

In the “Model Output” and “Recovery Output” rows, green dots (●) indicate actions with a training weight of 1, while red dots (●) indicate actions with a training weight of 0. \parallel and \square mean close and open, respectively. For close actions, we also annotate in the *Grasp Success* column whether the grasp is successful.

We label all actions from the moment the gripper is released to the moment it closes again and the grasp is determined to have failed as incorrect actions (●). All other actions are labeled as correct (●).

Status 2. Since the actions are labeled as incorrect, the data does not encourage the model to grasp at an incorrect location.

Status 3. The data encourages the model to attempt a grasp and move the gripper, even if it fails to grasp the garment — this movement is necessary for the model to visually determine whether the

Status	1. The gripper moves while grasping the garment.			2. The gripper opens and moves to next grasp point.			3. The gripper closes but fails to grasp the garment.			4. Open the gripper and reattempt the grasp.			5. Successful grasp, the model continues execution.		
Model Output	●	●	●	●	●	●	●	●	●				●	●	●
Recovery Output										●	●	●			
Gripper Action				□	□	□				□	□				
Grasp Success	✓	✓	✓				✗	✗	✗			✓	✓	✓	✓
Observation (Start)															
Observation (End)															

Figure 12: Keypoint-based recovery strategy.

grasp was successful. In our data generation process, the number of steps in this status is randomly sampled between 3 and 5.

Status 4. The data encourages the model to immediately release the gripper after detecting a grasp failure and then retry the grasp.

H Fold Policy Training Detail

We used a CNN-based policy from diffusion policy [37]. The observation encoder uses ResNet50, with the output observation feature dimension being 512. At the same time, we map the robot’s current state (the position of the left and right hand end-effectors in xyz coordinates and whether the grippers are open or closed) to a 512-dimensional space. The observation feature and the state feature are then concatenated together as the conditional input to the diffusion policy.

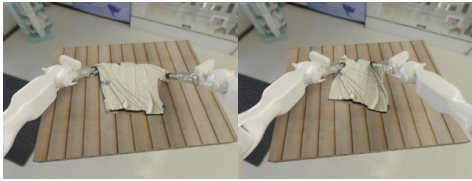
Parameter	Value
obs_horizon	1
state_horizon	1
action_predict_length	16
action_execute_length	4
action_repr	relative
image_size	(320, 240)
condition1d_unet_dims	(512, 1024, 2048)
num_parameters	279M
optimizer	AdamW
batch_size	256
learning_rate	1e-4

Table 5: Training hyperparameters.

Some training hyperparameters are listed in Table 5. Some of the hyperparameters may differ from those in the original paper. We compared the results of these modifications and ultimately selected the best-performing hyperparameters.

Depending on the amount of data and the specific task, the total number of training steps varies, ranging from approximately 100k to 400k. Training takes approximately one day on 8 NVIDIA RTX 4090 GPUs. We evaluate multiple checkpoints and select the best one.

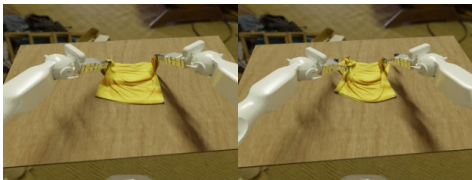
I Failure Mode in Simulation



Failure 1: The sleeves are not folded properly.



Failure 2: The sleeves are not folded properly.



Failure 3: The sleeves are not folded properly.



Failure 4: Unseen deformation.



Failure 5: Miss the garment bottom.



Failure 6: Miss the garment sleeves.



Failure 7: The bottom is over folded.



Failure 8: The bottom is not folded properly

Figure 13: Failure mode in simulation.

Figure 13 shows some typical failure cases in our simulation environment. In cases 1, 2, and 3, the model fails because it either does not grasp the correct position or fails to fold the clothes properly, resulting in the sleeves not being folded correctly. In case 4, the model attempts to fold the bottom of the clothes multiple times, leading to a deformation state that it has never encountered before, causing failure. In cases 5 and 6, even though the training data includes instances where the model needs to retry after failing to grasp, the model occasionally fails to recognize that the clothes are not grasped properly. In cases 7 and 8, the bottom of the clothes is either over folded or not folded correctly.

J Failure Mode in Real World

Figure 14 shows some typical failure cases in the real world. In the real world, there are some failure modes similar to those in simulation, such as 1, 2, and 3. However, some cases do not occur in simulation, such as case 4. The main reason for this is the significant sim2real gap in the modeling of the interaction between the clothes and the gripper in simulation.

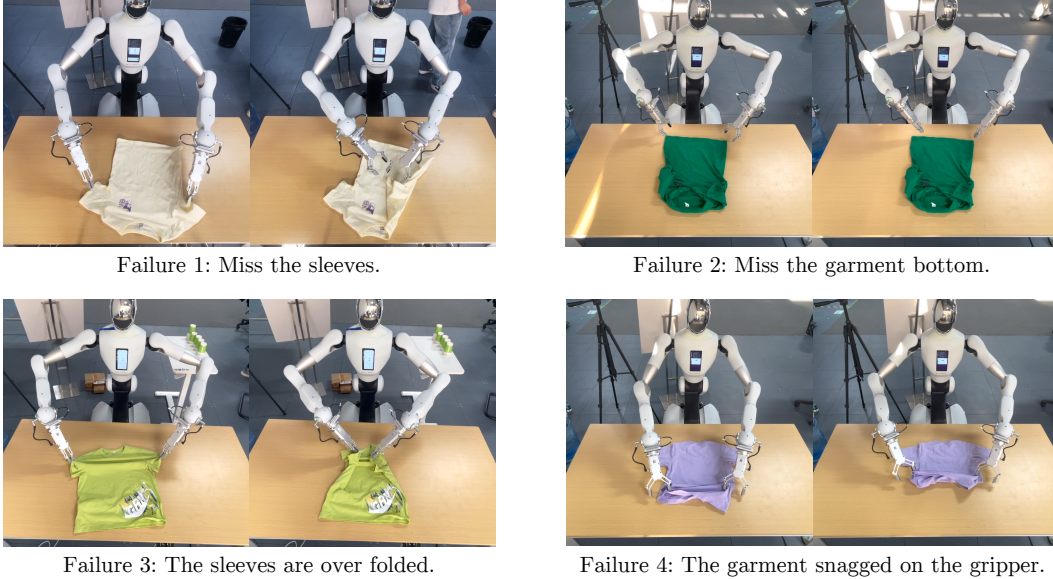


Figure 14: Failure mode in real world.

References

- [1] A. Longhini, Y. Wang, I. Garcia-Camacho, D. Blanco-Mulero, M. Moletta, M. Welle, G. Alenyà, H. Yin, Z. Erickson, D. Held, J. Borràs, and D. Kragic. Unfolding the literature: A review of robotic cloth manipulation, 2024. URL <https://arxiv.org/abs/2407.01361>.
- [2] M. Zare, P. M. Kebria, A. Khosravi, and S. Nahavandi. A survey of imitation learning: Algorithms, recent developments, and challenges. *IEEE Transactions on Cybernetics*, 54(12): 7173–7186, 2024. doi:10.1109/TCYB.2024.3395626.
- [3] J. Lu, W. Xia, D. Wang, Z. Wang, B. Zhao, D. Hu, and X. Li. Koi: Accelerating online imitation learning via hybrid key-state guidance. *arXiv preprint arXiv:2408.02912*, 2024.
- [4] H. Sikchi, C. Chuck, A. Zhang, and S. Niekum. A dual approach to imitation learning from observations with offline datasets, 2024. URL <https://arxiv.org/abs/2406.08805>.
- [5] G. Papagiannis and E. Johns. Miles: Making imitation learning easy with self-supervision, 2024. URL <https://arxiv.org/abs/2410.19693>.
- [6] Z. Zhou, A. Garg, D. Fox, C. Garrett, and A. Mandlekar. Spire: Synergistic planning, imitation, and reinforcement learning for long-horizon manipulation, 2024. URL <https://arxiv.org/abs/2410.18065>.
- [7] T. Ma, J. Zhou, Z. Wang, R. Qiu, and J. Liang. Contrastive imitation learning for language-guided multi-task robotic manipulation, 2024. URL <https://arxiv.org/abs/2406.09738>.
- [8] A. Canberk, C. Chi, H. Ha, B. Burchfiel, E. Cousineau, S. Feng, and S. Song. Cloth funnels: Canonicalized-alignment for multi-purpose garment manipulation. In *International Conference of Robotics and Automation (ICRA)*, 2022.
- [9] Y. Wang, Z. Sun, Z. Erickson, and D. Held. One policy to dress them all: Learning to dress people with diverse poses and garments, 2023. URL <https://arxiv.org/abs/2306.12372>.
- [10] J. Lyu, Y. Chen, T. Du, F. Zhu, H. Liu, Y. Wang, and H. Wang. Scissorbot: Learning generalizable scissor skill for paper cutting via simulation, imitation, and sim2real. In *8th Annual Conference on Robot Learning*, 2024.

- [11] H. Bertiche, M. Madadi, and S. Escalera. Cloth3d: clothed 3d humans. In *European Conference on Computer Vision*, pages 344–359. Springer, 2020.
- [12] B. Zhou, H. Zhou, T. Liang, Q. Yu, S. Zhao, Y. Zeng, J. Lv, S. Luo, Q. Wang, X. Yu, H. Chen, C. Lu, and L. Shao. Clothesnet: An information-rich 3d garment model repository with simulated clothes environment, 2023. URL <https://arxiv.org/abs/2308.09987>.
- [13] T. Lips, V.-L. D. Gusseme, and F. wyffels. Learning keypoints for robotic cloth manipulation using synthetic data, 2024. URL <https://arxiv.org/abs/2401.01734>.
- [14] H. Lu, R. Wu, Y. Li, S. Li, Z. Zhu, C. Ning, Y. Shen, L. Luo, Y. Chen, and H. Dong. Garmentlab: A unified simulation and benchmark for garment manipulation. In *Advances in Neural Information Processing Systems*, 2024.
- [15] Y. Li, J. Wu, R. Tedrake, J. B. Tenenbaum, and A. Torralba. Learning particle dynamics for manipulating rigid bodies, deformable objects, and fluids. *arXiv preprint arXiv:1810.01566*, 2018.
- [16] H. Xue, Y. Li, W. Xu, H. Li, D. Zheng, and C. Lu. Unifolding: Towards sample-efficient, scalable, and generalizable robotic garment folding, 2023. URL <https://arxiv.org/abs/2311.01267>.
- [17] Y. Avigal, L. Berscheid, T. Asfour, T. Kröger, and K. Goldberg. Speedfolding: Learning efficient bimanual folding of garments, 2022. URL <https://arxiv.org/abs/2208.10552>.
- [18] W. Chen, H. Xue, F. Zhou, Y. Fang, and C. Lu. Deformpam: Data-efficient learning for long-horizon deformable object manipulation via preference-based action alignment. *arXiv preprint arXiv:2410.11584*, 2024.
- [19] T. Tian, H. Li, B. Ai, X. Yuan, Z. Huang, and H. Su. Diffusion dynamics models with generative state estimation for cloth manipulation, 2025. URL <https://arxiv.org/abs/2503.11999>.
- [20] H. Jiang, H.-Y. Hsu, K. Zhang, H.-N. Yu, S. Wang, and Y. Li. Phystwin: Physics-informed reconstruction and simulation of deformable objects from videos, 2025. URL <https://arxiv.org/abs/2503.17973>.
- [21] S. Miller, M. Fritz, T. Darrell, and P. Abbeel. Parametrized shape models for clothing. In *2011 IEEE International Conference on Robotics and Automation*, pages 4861–4868, 2011. doi:10.1109/ICRA.2011.5980453.
- [22] K. Youwang, T.-H. Oh, and G. Pons-Moll. Paint-it: Text-to-texture synthesis via deep convolutional texture map optimization and physically-based rendering. In *IEEE Conference on Computer Vision and Pattern Recognition (CVPR)*, 2024.
- [23] D. Z. Chen, Y. Siddiqui, H.-Y. Lee, S. Tulyakov, and M. Nießner. Text2tex: Text-driven texture synthesis via diffusion models, 2023. URL <https://arxiv.org/abs/2303.11396>.
- [24] B. Wen, W. Yang, J. Kautz, and S. Birchfield. Foundationpose: Unified 6d pose estimation and tracking of novel objects, 2024. URL <https://arxiv.org/abs/2312.08344>.
- [25] P. Sundaresan, Q. Vuong, J. Gu, P. Xu, T. Xiao, S. Kirmani, T. Yu, M. Stark, A. Jain, K. Hausman, D. Sadigh, J. Bohg, and S. Schaal. Rt-sketch: Goal-conditioned imitation learning from hand-drawn sketches, 2024. URL <https://arxiv.org/abs/2403.02709>.
- [26] J. Hejna, C. Bhateja, Y. Jiang, K. Pertsch, and D. Sadigh. Re-mix: Optimizing data mixtures for large scale imitation learning, 2024. URL <https://arxiv.org/abs/2408.14037>.

- [27] X. Jia, Q. Wang, A. Donat, B. Xing, G. Li, H. Zhou, O. Celik, D. Blessing, R. Lioutikov, and G. Neumann. Mail: Improving imitation learning with mamba, 2024. URL <https://arxiv.org/abs/2406.08234>.
- [28] V. Myers, B. C. Zheng, O. Mees, S. Levine, and K. Fang. Policy adaptation via language optimization: Decomposing tasks for few-shot imitation, 2024. URL <https://arxiv.org/abs/2408.16228>.
- [29] T. Z. Zhao, J. Tompson, D. Driess, P. Florence, K. Ghasemipour, C. Finn, and A. Wahid. Aloha unleashed: A simple recipe for robot dexterity, 2024. URL <https://arxiv.org/abs/2410.13126>.
- [30] C. Chi, Z. Xu, C. Pan, E. Cousineau, B. Burchfiel, S. Feng, R. Tedrake, and S. Song. Universal manipulation interface: In-the-wild robot teaching without in-the-wild robots, 2024. URL <https://arxiv.org/abs/2402.10329>.
- [31] X. Yuan, T. Mu, S. Tao, Y. Fang, M. Zhang, and H. Su. Policy decorator: Model-agnostic online refinement for large policy model, 2024. URL <https://arxiv.org/abs/2412.13630>.
- [32] M. Kelly, C. Sidrane, K. Driggs-Campbell, and M. J. Kochenderfer. Hg-dagger: Interactive imitation learning with human experts, 2019. URL <https://arxiv.org/abs/1810.02890>.
- [33] Y. Jiang, C. Wang, R. Zhang, J. Wu, and L. Fei-Fei. Transic: Sim-to-real policy transfer by learning from online correction. In *Conference on Robot Learning*, 2024.
- [34] J. Luo, C. Xu, J. Wu, and S. Levine. Precise and dexterous robotic manipulation via human-in-the-loop reinforcement learning, 2024.
- [35] OpenAI. Gpt-4o system card, 2024. URL <https://arxiv.org/abs/2410.21276>.
- [36] D. Podell, Z. English, K. Lacey, A. Blattmann, T. Dockhorn, J. Müller, J. Penna, and R. Rombach. Sdxl: Improving latent diffusion models for high-resolution image synthesis, 2023. URL <https://arxiv.org/abs/2307.01952>.
- [37] C. Chi, S. Feng, Y. Du, Z. Xu, E. Cousineau, B. Burchfiel, and S. Song. Diffusion policy: Visuomotor policy learning via action diffusion. In *Proceedings of Robotics: Science and Systems (RSS)*, 2023.
- [38] Blender Foundation. Blender. URL <https://www.blender.org>.
- [39] T. Ren, S. Liu, A. Zeng, J. Lin, K. Li, H. Cao, J. Chen, X. Huang, Y. Chen, F. Yan, Z. Zeng, H. Zhang, F. Li, J. Yang, H. Li, Q. Jiang, and L. Zhang. Grounded sam: Assembling open-world models for diverse visual tasks, 2024.
- [40] PolyHaven Team. Poly haven - the public 3d asset library. URL <https://polyhaven.com/>.
- [41] O. Ronneberger, P. Fischer, and T. Brox. U-net: Convolutional networks for biomedical image segmentation, 2015. URL <https://arxiv.org/abs/1505.04597>.
- [42] Z. Tu, H. Talebi, H. Zhang, F. Yang, P. Milanfar, A. Bovik, and Y. Li. Maxvit: Multi-axis vision transformer, 2022. URL <https://arxiv.org/abs/2204.01697>.
- [43] R. Wightman. Pytorch image models. <https://github.com/rwightman/pytorch-image-models>, 2019.